CO_2 HYDROGENATION OVER CERIA-BASED TRANSITION METAL NANOCATALYSTS

S. Stefa[1], G. Varvoutis[2,3], M. Lykaki[4], V. Binas[1,5], G.E. Marnellos[6,7], M. Konsolakis[4,*]

[1]Institute of Electronic Structure and Laser, Foundation for Research and Technology-Hellas (FORTH-IESL), Heraklion, Greece

[2]Department of Mechanical Engineering, University of Western Macedonia, Kozani, Greece

[3]Cluster of Bioeconomy and Environment of Western Macedonia, Kozani, Greece

[4]School of Production Engineering & Management, Technical University of Crete, Chania, Greece

[5]Department of Chemistry, Aristotle University of Thessaloniki, Thessaloniki, Greece

[6]Department of Chemical Engineering, Aristotle University of Thessaloniki, Thessaloniki, Greece

[7]Chemical Process and Energy Resources Institute, Centre for Research & Technology Hellas, Thermi, Greece

(*mkonsolakis@tuc.gr)

ABSTRACT

The hydrogenation of CO_2 to value-added products by means of green H_2 has gained increasing attention for mitigating CO_2 emissions and utilizing the excess power of renewable energy sources. Ceria-based transition metal catalysts have received significant attention due to their intrinsic properties in conjunction with their lower cost as compared to noble metal-based catalysts. In the present work, CO_2 hydrogenation is explored over a series of M/CeO_2-NR catalysts, employing first row 3d transition metals (Ti, V, Cr, Mn, Fe, Co, Ni, Cu, Zn) as the active metal phases and rod-shaped ceria as support. The as-prepared materials were thoroughly characterized by various complementary characterization techniques, involving N_2 adsorption at –196 °C, XRD, SEM/EDS, TEM, TPR, and were catalytically evaluated under stoichiometric reaction conditions (H_2/CO_2 = 4). It is worth mentioning that a volcano-type dependence of CO_2 hydrogenation activity and selectivity was disclosed as a function of metal entity (Ti – Zn) revealing a maximum for the Ni-based sample. According to the catalytic results, the CO_2 conversion performance of M/CeO_2-NR catalysts is strongly dependent on the metal entity, following the trend: Ni > Co > Cu > Fe > Zn > Cr ≈ Ti ≈ V ≈ Mn. In particular, Ni/CeO_2-NR exhibits by far the best performance, offering ~90% conversion at 300 °C. Moreover, all the M/CeO_2-NR systems, except those of Ni and Co, are mainly selective to CO. Both the CO_2 hydrogenation activity and selectivity can be closely related to the intrinsic features of each metal in relation to its ability to activate CO_2 and dissociate H_2. The catalytic evaluation of the as-prepared samples in rWGS and CO_2 methanation constitutes the stepping stone for their further assessment towards the production of olefins.

KEYWORDS: CO_2 hydrogenation, transition metals, ceria nanorods

INTRODUCTION

Carbon dioxide (CO_2), mainly originated from fossil fuel energy sources, is a major contributor to the accumulation of greenhouse gases. In order to mitigate greenhouse gas emissions, it is of great significance to optimize the utilization of fossil fuels and implement effective Carbon Capture and Utilization (CCU) technologies [1,2]. A sustainable CCU strategy is CO_2 hydrogenation, in which captured CO_2 is reduced through its reaction with hydrogen. Under atmospheric pressure conditions, this can be achieved by either the reverse water-gas shift (rWGS) reaction (Eq. 1), which produces CO or the methanation reaction (Eq. 2), which yields CH_4 [3].

$$CO_2 + H_2 \leftrightarrow CO, \Delta H = +41.3\ KJ/mol \quad (1)$$

$$CO_2 + 4H_2 \leftrightarrow CH_4 + 2H_2O, \Delta H = -164.7\ \mathrm{KJ/mol} \quad (2)$$

Among the investigated oxide materials, ceria (CeO_2) has gained significant attention as support due to its exceptional properties such as oxygen storage capacity, oxygen mobility, strong metal-support interactions, and rapid exchange between its two oxidation states (Ce^{3+}/Ce^{4+}) [4–6]. Besides the excellent catalytic activity of ceria-based noble metals (Ru, Rh, Pd), their high cost and limited availability render them undesirable from a techno-economic point of view. In view of this context, recent research efforts have focused on the rational design of cost-efficient and highly-active non-noble metal catalysts, emphasizing on the 3d transition metals (TMs), which can adequately adsorb and activate CO_2 molecules [6–8]. To this direction, we recently showed that Ni catalysts supported on rod-shaped ceria nanoparticles exhibit excellent hydrogenation performance, attributed mainly to the enhanced redox properties of ceria nanorods in conjunction to the synergistic nickel-ceria interactions [6,9,10]. Moreover, Cu/CeO_2 sample of rod-like morphology demonstrates excellent rWGS performance, revealing the key role of metal entity in CO_2 adsorption/activation and in turn in activity and selectivity towards CO or CH_4 [11,12]. In the present study, a series of M/CeO_2 catalysts with a constant atomic ratio of M/Ce = 0.25 were prepared, using the first row 3d transition metals (Ti, V, Cr, Mn, Fe, Co, Ni, Cu, Zn) as active phases for ceria nanorods (CeO_2-NR). The catalytic materials were thoroughly characterized by various techniques (N_2 adsorption at –196 °C, XRD, SEM/EDS, TEM, H_2-TPR). The catalytic evaluation of the as-prepared samples in rWGS and CO_2 methanation will act as the onset for their further assessment towards olefins production.

METHODOLOGY

Bare ceria nanorods (CeO_2-NR) were synthesized through the hydrothermal method, as thoroughly described in our previous work [13]. Ceria-based transition metals (M/CeO_2, TM: Ti, V, Cr, Mn, Fe, Co, Ni, Cu) were synthesized by the wet impregnation method, using aqueous solutions of metal nitrate precursors, so as to obtain a M/Ce atomic ratio of 0.25. The obtained suspensions were heated under stirring until water evaporation, dried at 90 °C for 12 h, and finally calcined at 500 °C for 2 h (heating ramp 5 °C/min) [10].

The catalytic materials were thoroughly characterized in terms of their textural (N_2 adsorption at –196 °C), structural (XRD), morphological (SEM/EDS, TEM) and redox (H_2-TPR) properties.

Catalytic studies were carried out in a quartz fixed-bed U-shaped reactor (i.d. = 1 cm), loaded with 200 mg of catalyst diluted with 200 mg of inert SiO_2. The samples were reduced in situ at 400 °C for 1 h under pure H_2 flow (40 $cm^3\ min^{-1}$), followed by flushing with He (10 $cm^3\ min^{-1}$) until room temperature. The experiments were conducted at 1 bar and in the temperature range of 200 – 500 °C at intervals of 15–20 °C and a heating rate of 1 °C/min. The total volumetric feed flow was 100 $cm^3\ min^{-1}$, corresponding to a weight hourly space velocity (WHSV) of 30 $L \cdot g^{-1} \cdot h^{-1}$. The gas feed constituted of a H_2/CO_2 mixture at a molar ratio of 4.

RESULTS AND DISCUSSION

The main textural and structural characteristics of bare CeO_2-NR and M/CeO_2 samples (atomic ratio M/Ce = 0.25) are summarized in Table 1. Bare ceria demonstrates a BET surface area of 79 m^2/g while the addition of the transition metals into CeO_2 slightly decreases the BET surface area.

Table 1. *Textural and structural characteristics of CeO_2 and M/CeO_2 samples.*

Sample	Nominal metal loading (wt%)	EDS analysis		BET analysis	XRD analysis		TEM analysis
		Atomic ratio M/Ce	Metal content (wt%)	SBET (m^2/g)	Average crystallite size (nm)		M_xO_y particle size (nm)
					CeO_2	M_xO_y	
CeO_2-NR	–	–	–	79	15	–	–
Ti/CeO_2	6.5	0.24	6.3	–	11	20	16
V/CeO_2	6.9	0.28	7.6	–	14	45	28
Cr/CeO_2	7.0	0.26	7.2	–	11	–	10
Mn/CeO_2	7.4	0.22	6.5	–	11	–	15
Fe/CeO_2	7.5	0.21	6.3	69	10	7	11
Co/CeO_2	7.9	0.26	8.1	72	14	16	15
Ni/CeO_2	7.9	0.25	7.8	72	14	23	10
Cu/CeO_2	8.5	0.25	8.6	75	12	43	16
Zn/CeO_2	8.7	0.24	8.3	76	12	44	41

The XRD patterns of bare CeO_2-NR and M/CeO_2 samples are presented in Figure 1. The main diffraction peaks of ceria nanorods correspond to the face-centered cubic (fcc) fluorite structure of ceria (Fm3m symmetry, no. 225) [14]. Furthermore, the diffractions peaks of M/CeO_2 samples (M: Ti, Fe, Co, Ni, Cu, Zn) show the existence of TiO_2, Fe_2O_3, Co_3O_4, NiO, CuO, ZnO, respectively, apart from ceria. The Mn/CeO_2 and Cr/CeO_2 samples do not exhibit any diffraction peaks, except from ceria. In the V/CeO_2 sample, the diffraction peaks detected are attributed to the CeO_2 and $CeVO_4$ crystal phases.

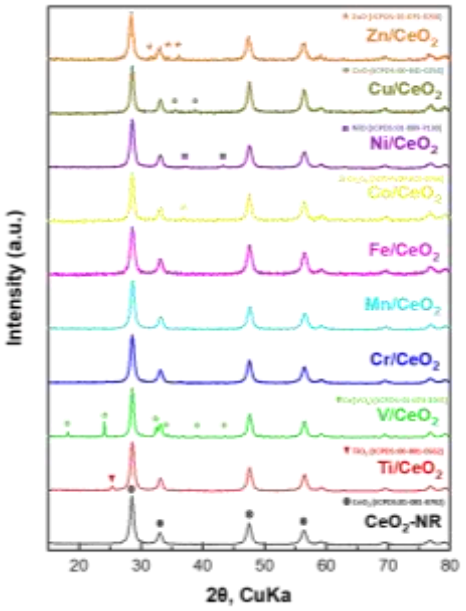

Figure 1. *XRD patterns of CeO_2-NR and M/CeO_2 samples.*

The morphological characteristics of the samples were analyzed by TEM, as shown in Figure 2. It is obvious that ceria support retains its nanorod morphology upon addition of the metal entity.

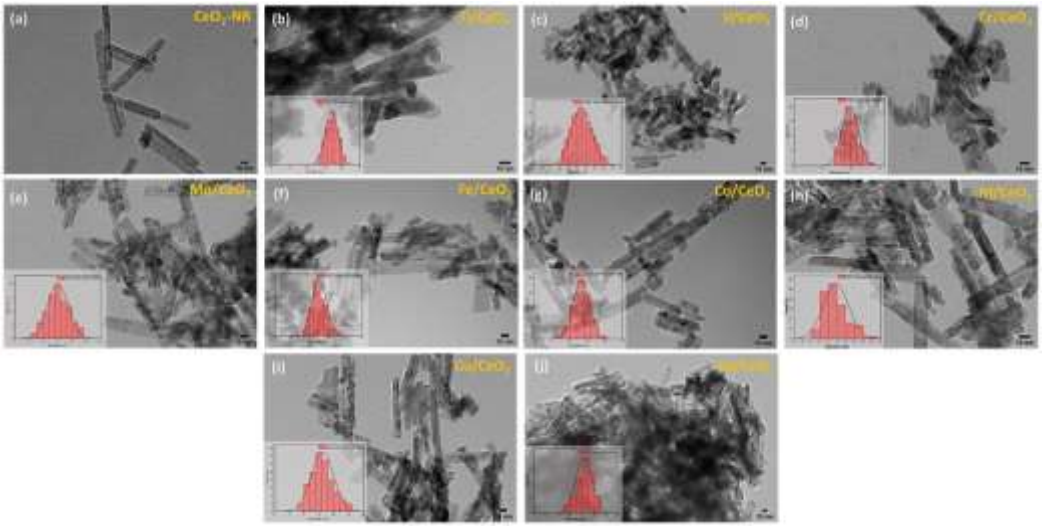

Figure 2. *TEM images of the samples: (a) CeO_2-NR, (b) Ti/CeO_2, (c) V/CeO_2, (d) Cr/CeO_2, (e) Mn/CeO_2, (f) Fe/CeO_2, (g) Co/CeO_2, (h) Ni/CeO_2, (i) Cu/CeO_2, and (j) Zn/CeO_2.*

For the optimum catalytic systems (Ni/CeO_2 and Co/CeO_2 for CO_2 methanation, Fe/CeO_2 and Cu/CeO_2 for the rWGS reaction), TPR measurements were performed in the temperature range of 100–1000 °C, using H_2 as reducing agent, in order to gain insight into the impact of metal entity on the reducibility. As depicted in Figure 3, bare CeO_2-NR exhibits two broad reduction peaks, attributed to the surface (O_s) and bulk (O_b) oxygen reduction of ceria, respectively [15]. The addition of the metal phase facilitates ceria surface oxygen reduction with all M/CeO_2 samples exhibiting a high-temperature peak in the range of 747–793 °C which is attributed to the ceria sub-surface oxygen reduction.

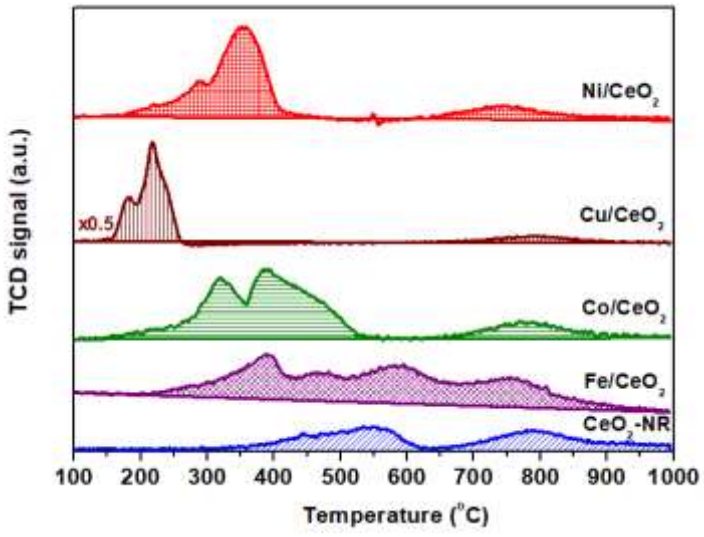

Figure 3. *H_2-TPR profiles of CeO_2-NR and representative M/CeO_2 samples.*

In Figure 4, CO_2 conversion and CO selectivity in the temperature range of 200–500 °C are depicted for all M/CeO_2 samples. Apparently, the conversion of CO_2 depends strongly on the metal entity, following the general trend: Ni > Co > Cu > Fe > Zn > Cr ≈ Ti ≈ V ≈ Mn, with the Ni/CeO_2 catalyst exhibiting the optimum performance (~90% conversion at 300 °C). Also, the early 3d transition metals (Ti, V, Cr, Mn) are almost inactive (X_{CO2} < 10% at T < 400 °C), demonstrating even lower

conversion performance than bare ceria nanorods. All M/CeO_2 systems, apart from Ni and Co, are mainly selective to CO. In particular, the Ni/CeO_2 catalyst is completely selective to CH_4 in the whole temperature range, whereas the Co/CeO_2 sample exhibits intermediate selectivity values depending on temperature.

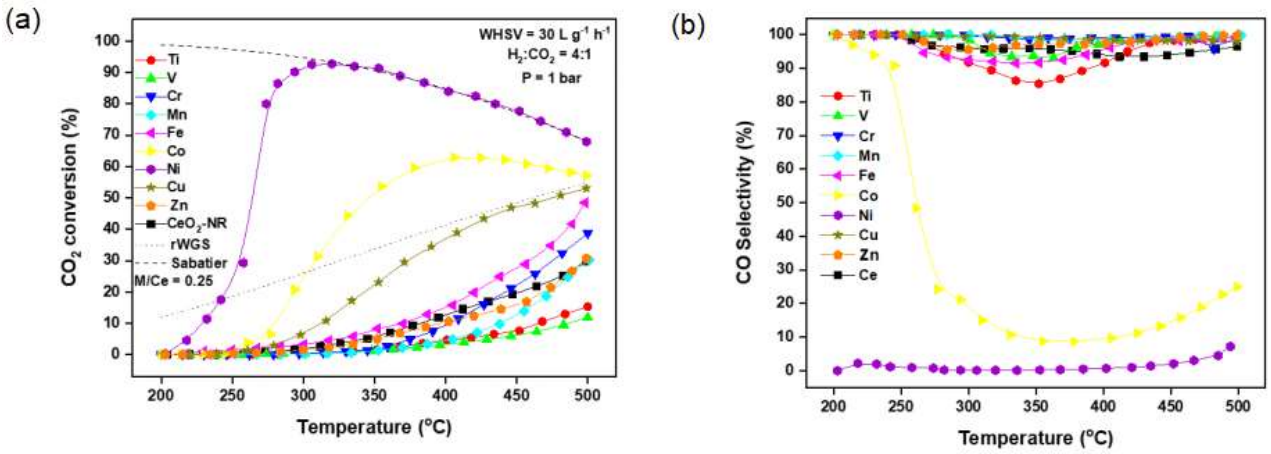

***Figure 4**. CO_2 conversion (a) and CO selectivity (b) for the first row 3d transition metals supported on CeO_2 nanorods. Reaction conditions: WHSV = 30 $L \cdot g^{-1} \cdot h^{-1}$, $H_2:CO_2 = 4$, P = 1 bar.*

In order to gain insight into the role of metal entity in CO_2 hydrogenation performance, the normalized reaction rate of CO_2 consumption (r_{CO2}) and the selectivity to methane (S_{CH4}) were plotted at a specific reaction temperature (350 °C), as shown in Figure 5. Notably, a volcano-shaped dependence of CO_2 conversion and CH_4 selectivity was disclosed for the first row 3d transition metals, (Ti, V, Cr, Mn, Fe, Co, Ni, Cu, Zn) with a maximum obtained for Ni. Particularly, Ni/CeO_2 exhibits the optimum hydrogenation performance in terms of CO_2 consumption rate (~800 µmol $g_{Ni}^{-1}s^{-1}$) and CH_4 selectivity (100%), followed by Co (r_{CO2} = 445.44 µmol $g_{Co}^{-1}s^{-1}$, S_{CH4} = 90%). The 3d early transition metals (Ti – Fe), as well as the 3d late metals (Cu and Zn), exhibit much lower reactivity (r_{CO2} < 200 µmol $g_M^{-1}s^{-1}$), while being selective to CO (Figure 4).

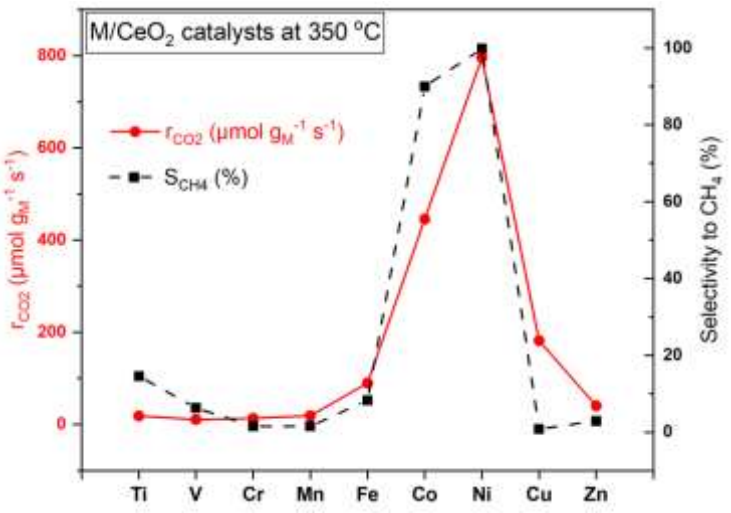

***Figure 5.** Metal entity-dependence of CO_2 conversion and CH_4 selectivity at 350 °C for the first row 3d transition metals supported on ceria nanorods.*

In this point, it ought to be mentioned that the present experimental findings (Figure 5) agree perfectly with the theoretically predicted trend for CO_2 hydrogenation following the formate

pathway, as revealed by Sun et al. [16], thus indicating the prevalence of formate route and the significance of energy barrier for CO_2 activation and H_2 dissociation.

CONCLUSIONS

In the present work, a series of M/CeO_2 catalysts (atomic ratio M/Ce = 0.25) were catalytically evaluated in CO_2 hydrogenation, employing the first row 3d transition metals (Ti, V, Cr, Mn, Fe, Co, Ni, Cu, Zn) as active phases. The Ni/CeO_2 sample demonstrated its superiority in terms of CO_2 conversion rate (~800 μmol $g_{Ni}^{-1}s^{-1}$) and CH_4 selectivity (100%), followed by Co (r_{CO2} = 445.44 μmol $g_{Co}^{-1}s^{-1}$, S_{CH4} = 90%). The 3d early transition metals (Ti – Fe) and the 3d late metals (Cu and Zn) exhibit much lower activity (r_{CO2} < 200 μmol $g_M^{-1}s^{-1}$), while being selective to CO. Notably, the key role of metal entity in CO_2 hydrogenation was clearly established, as illustrated by the volcano-shaped dependence of both activity and selectivity to methane as a function of 3d-orbital electron number, with Ni located at the peak of this volcano curve. The present experimental findings concerning the CO_2 hydrogenation performance over ceria-based transition metal catalysts constitute an adequate overview for their further assessment towards olefins production.

ACKNOWLEDGEMENTS

This research has received funding from the European Union under grant agreement No 101099717 – ECOLEFINS project. Views and opinions expressed are however those of the author(s) only and do not necessarily reflect those of the European Union or European Innovation Council and SMEs Executive Agency (EISMEA) granting authority. Neither the European Union nor the granting authority can be held responsible for them.

REFERENCES

[1] Atsbha TA, Yoon T, Seongho P, Lee CJ. (2021). *J. CO_2 Util.,* 44, 101413.
[2] Wang H, Liu Y, Laaksonen A, Krook-Riekkola A, Yang Z, Lu X, Ji X. (2020). *Renew. Sustain. Energy Rev.,* 131, 110010.
[3] Romeo LM, Bailera M. (2020). *J. CO_2 Util.,* 39, 101174.
[4] Ebrahimi P, Kumar A, Khraisheh M. (2022). *Catalysts,* 12, 1101.
[5] Hussain I, Tanimu G, Ahmed S, Aniz CU, Alasiri H, Alhooshani K. (2023). *Int. J. Hydrogen Energy,* 48, 24663–24696.
[6] Konsolakis M, Lykaki M. (2021). *Catalysts,* 11, 452.
[7] Konsolakis M, Lykaki M. (2020). *Catalysts,* 10, 160.
[8] Li Y, Zhang X, Zheng Z. (2022). *CCS Chem.,* 4, 31–53.
[9] Varvoutis G, Lykaki M, Stefa S, Binas V, Marnellos GE, Konsolakis, M. (2021). *Appl. Catal. B: Environ.,* 297, 120401.
[10] Varvoutis G, Lykaki M, Stefa S, Papista E, Carabineiro SAC, Marnellos GE, Konsolakis M. (2020). *Catal. Commun.,* 142, 106036.
[11] Konsolakis M, Lykaki M, Stefa S, Carabineiro SAC, Varvoutis G, Papista E, Marnellos GE. (2019). *Nanomaterials,* 9, 1739.
[12] Varvoutis G, Lykaki M, Marnellos GE, Konsolakis M. (2023). *Catalysts,* 13, 275.
[13] Lykaki M, Pachatouridou E, Carabineiro SAC, Iliopoulou E, Andriopoulou C, Kallithrakas-Kontos N, Boghosian S, Konsolakis M. (2018). *Appl. Catal. B: Environ.,* 230, 18–28.
[14] Sebastian R, Swapna MS, Sankararaman S. (2020). *SN Appl. Sci.,* 2, 1145.
[15] Rao GR. (1999). *Bull. Mater. Sci.,* 22, 89–94.
[16] Sun J, Zhao H, Fang X, Zhai S, Zhai D, Sun L, Deng W. (2021). *Mol. Catal.,* 508, 111581.